Biophysical Journal Volume 82 March 2002 1460–1468

# Molecular Dynamics Simulation of Proton Transport Near the Surface of a Phospholipid Membrane

Alexander M. Smondyrev and Gregory A. Voth
Department of Chemistry and Henry Eyring Center for Theoretical Chemistry, University of Utah, Salt Lake City, Utah 84112-0850 USA

ABSTRACT The structural and dynamical properties of a hydrated proton near the surface of DMPC membrane were studied using a molecular dynamics simulation. The proton transport between water molecules was modeled using the second generation multistate empirical valence bond model. The proton diffusion was found to be inhibited at the membrane surface. The potential of mean force for the proton adsorption to the membrane surface and its release back into the bulk water was also determined, yielding a small barrier in each direction. An efficient algorithm for Ewald summation calculations for the multistate empirical valence bond model is also introduced.

## INTRODUCTION

Proton transport is important for a number of biological functions. For example, it has been suggested to play a central role in bioenergetics, such as the light-induced proton pumping in bacteriorhodopsin (BR) and the subsequent ATP and NADPH generation in higher plants and algae (Mathies et al., 1991). The electrochemical gradient of $H^+$ ions across the membrane in mitochondria is also essential for the energy yielding reactions during the respiratory cycle driving the synthesis of ATP from ADP and $P_i$ (Malmstrom, 1989; Futai et al., 1989). Ion channels formed by integral transmembrane proteins can also enable protons to move across the membrane (Nagle and Tristram-Nagle, 1983; Heberle, 2000; Brandsburg-Zabary et al., 2000). This mechanism is important in a number of processes, such as cell signaling and in helping to maintain the appropriate cellular environment. For example, the proton transport through the M2 channel of the influenza A virus has been implicated in the viral replication (Sugrue and Hay, 1991). Another example of a proton conducting channel is gramicidin A (Dubos and Hotchkiss, 1941), where the proton hops through a single-file chain of water molecules via a Grotthuss mechanism (for discussion, see Agmon, 1995).

Proton release from the the generator, such as BR, into the extracellular space is only the first step in a number of complex reactions occurring at the membrane surface. The subsequent proton migration along or near the membrane surface to the active sites plays an important role in determining the reaction rates. An example of such a process is the release of protons onto the membrane surface by BR and its consumption in $H^+$ − ATP synthase. In this context the understanding of proton mobility and their interactions with membrane surfaces becomes important.

Yet another example of a system where the proton diffusion along the membrane surface may be a limiting process is the example of proton transport through water wires spanning lipid membranes (Nagle and Dilley, 1986; Marrink et al., 1996). The life time of such chains in molecular dynamics (MD) simulations has been found to be sufficient for a single proton transfer event. However, at normal physiological conditions it was estimated that the limiting step for the proton transport process through the membrane may be the rate at which a proton is first delivered to a given transmembrane water chain (Deamer, 1996).

Measurements of proton migration have been performed using pH sensitive dyes, which allow one to study the proton transfer along the membrane surface and into the bulk solvent by placing probes at selected positions (Heberle and Dencher, 1992; Heberle et al., 1994; Gutman et al., 1992; Scherrer et al., 1994; Nachliel and Gutman, 1996). It was suggested that the proton transfer from the membrane surface into the bulk is retarded, resulting in relative long dwell times for the proton near the membrane surface. As the proton dwell time at the membrane surface becomes sufficiently long, the proton may diffuse long distances between proton generators and consumers. In this case experimental data may be explained without assuming that the proton diffusion is much faster than in bulk water. At the same time it was also suggested that the proton may exhibit fast diffusion in a two-dimensional layer at the membrane water interface, which might be due to the ordering of water molecules near the membrane surface. The water molecules in this layer might become less mobile translationally, but they could exhibit faster orientational motions thus promoting the proton diffusion. It therefore seems probable that any proton translocation using hydrogen bond networks (as in a Grotthuss-type mechanism) along the membrane surface would depend on the membrane composition.

The modeling of proton transport is impossible using conventional MD force fields. First principles molecular dynamics simulations, which use the Car-Parrinello ap-

*Submitted November 21, 2001, and accepted for publication December 5, 2001.*

Address reprint requests to Gregory Voth, Department of Chemistry, Henry Eyring Center for Theoretical Chemistry, University of Utah, 315 S. 1400 E., Room 2020, Salt Lake City, UT 84112-0850. Tel.: 801-581-7272; Fax: 801-581-4353; E-mail: voth@chem.utah.edu.



0006-3495/02/03/1460/09 $2.00

proach (Car and Parrinello, 1985) can instead be used to study processes involving bond dissociation. However, such a methodology is limited to studies of small systems consisting of several tens of molecules (Marx et al., 1999) and short trajectories, given its computational cost. Extension of these methods to biologically relevant systems is therefore limited due to this issue unless additional approximations are introduced.

Recently, however, Schmitt and Voth have built upon the original two-state by Lobaugh and Voth (1996) and developed a multi-state empirical valence bond model (MS-EVB) (Schmitt and Voth, 1998, 1999a,b; Brewer et al., 2001), which can be incorporated into conventional MD simulations. It was shown that this potential can successfully reproduce various important features of the excess proton in bulk water, such as the proton hopping rate and the density of vibrational states. The model also provides a good description of the relative stability of the solvated Eigen and Zundel species (Marx et al., 1999). The MS-EVB approach was further applied to study proton wire dynamics in a model channel environment (Brewer et al., 2001). The next generation of the MS-EVB model, which will be called here MS-EVB2 (Cuma et al., 2001; Day and Voth, unpublished data), has recently been developed, along with an extension of the approach to treat acid-base equilibria (Cuma et al., 2001).

Several other models for the hydrated proton have also been proposed. For example, an alternative multi-state model was developed by Borgis and co-workers (Vuilleumier and Borgis, 1997, 1998a,b, 1999), which also extended the original Lobaugh-Voth two-state EVB model, while Zahn and Brickmann proposed a two-state quantum-classical method to describe proton migration in water (Zahn and Brickmann, 2001). Walbran and Kornyshev (2001) have also proposed a different model using a hybrid "switching function" and two-state EVB force field, whereas Lill and Helms (2001) have developed a nondeterministic approach to modeling proton hopping in MD simulations. A combined MD and diffusion model was also introduced by Schumaker et al. (2000, 2001) to predict the conductance properties of the gramicidin channel. Because it is not the focus of this paper, it is left to the reader to compare the various strengths and weaknesses of these alternative models with the MS-EVB approach.

The aim of this work is to study proton transport near the membrane interface using the MS-EVB2 model. Properties of water near the membrane surface vary significantly from those observed for bulk water due to the presence of polar lipid headgroups. The hydrogen bonding of water molecules also changes around lipid molecules as water molecules can form direct hydrogen bonds with lipid atoms and form water bridges linking adjacent lipids. The membrane electrostatic potential may also have a pronounced effect on the proton diffusion. The present paper will only report MD simulations on the effect of the membrane environment on the proton transfer between water molecules. Future work will be concerned with the aspects of proton transport across membranes, as well as the role of the protonation/deprotonation of lipid headgroups in the transport process.

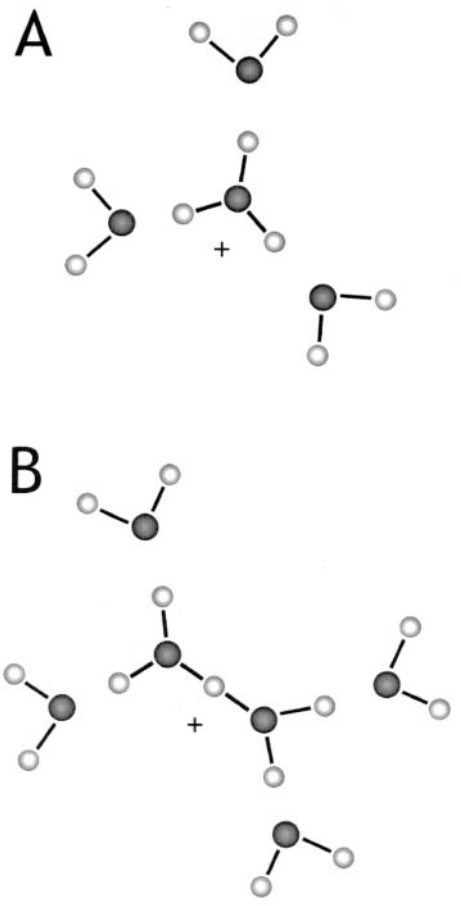


FIGURE 1 Schematic pictures of the Eigen cation $H_9O_4^+$ (*A*) and the solvated Zundel cation $H_5O_2^+$.

## MATERIALS AND METHODS

The model membrane consisted of 64 dipalmitoylphosphatidylcholine (DMPC) molecules hydrated by 1312 waters, corresponding to 20.5 water molecules per lipid, which is close to full hydration in MLVs (Nagle and Weiner, 1988). Several initial configurations for the simulations were taken from an equilibrium molecular dynamics trajectory of the DMPC bilayer in water (Smondyrev and Berkowitz, 1999a). An excess proton was then added at different positions within the solvent layer. This was done by replacing a random water molecule with a hydronium ($H_3O^+$) cation. Each system was then allowed to equilibrate for 20 ps using standard classical MD (no proton transfer between water molecules was allowed at this stage), which was followed by longer production runs using the MS-EVB approach, which is described in greater details elsewhere (Schmitt and Voth, 1998, 1999a,b).

Here we present only a brief description of essential features of the MS-EVB approach. At each MD step one constructs a number of possible EVB states. Each of those states consists of a hydronium cation and *n* water molecules. For example, in the gas phase, the Zundel cation $H_5O_2^+$ is represented by two EVB states, whereas four EVB states are required to

represent an Eigen cation $H_9O_4^+$ (see Fig. 1). An empirical valence bond potential can then be used to construct a ($N \times N$) Hamiltonian matrix $H$, such that the ground state potential energy ($E_0$) is given by:

$$c^{\mathrm{T}}Hc = E_0,$$

in which $c$ is the ground state eigenvector. The "pivot" hydronium for the EVB state selection process is determined based on the state with the highest probability $c_i^2$ from the set of eigenvectors. The off-diagonal elements of the Hamiltonian matrix are defined to reproduce various important properties of the system such as cluster energies, geometries, and proton transfer barriers. After determining the MS-EVB Hamiltonian matrix and ground state eigenvector, forces can be calculated using the Hellmann-Feynman theorem:

$$F_i = -\left\langle \Psi_0 \left| \frac{\partial H}{\partial x_i} \right| \Psi_0 \right\rangle = -\sum_{m,n} c_m^0 c_n^0 \frac{\partial}{\partial x_i} h_{mn}(x),$$

in which $h_{mn}(x)$ are the elements of MS-EVB Hamiltonian matrix and $x$ represents all system coordinates. The interactions between hydronium and surrounding water molecules were modeled here using the MS-EVB2 parameter set (Cuma et al., 2001; Day and Voth, unpublished data) developed for the hydrated proton in bulk water.

In the present work, proton transfer between water and DMPC molecules was not allowed. The effect of such protonation/deprotonation of the polar headgroups is unclear. On one hand, it might serve to stabilize the excess protons and hence inhibit transport. On the other hand, such processes might work in concert with hydrogen bonding rearrangements to facilitate the proton transport. Clearly, this process will be an important topic for future research.

United atom force field parameters (Smondyrev and Berkowitz, 1999b) were used to define the potential function of the DMPC molecules. The water molecules were modeled using the modified flexible TIP3P potential (Dang and Pettitt, 1987). DMPC bonds were constrained using the SHAKE algorithm (Ryckaert et al., 1977) with a tolerance of $10^{-4}$. The water bonds were flexible and the equations of motion were integrated using a timestep of 1 fs, which is consistent with the water hydrogen vibrational modes. Simulations were performed at constant volume and temperature ($T = 308$ $K$), which is above the main transition temperature ($T_m = 293$ K) for fully hydrated DMPC bilayers. Temperature was controlled using the Nose-Hoover thermostat (Hoover, 1985) with a thermostat relaxation time of 0.2 ps. Electrostatic interactions were calculated using Ewald summation technique with a tolerance of $10^{-4}$. The real-space part of the Ewald sum and short range van der Waals forces were truncated at 10 Å. Periodic boundary conditions were applied in all directions. An efficient Ewald summation algorithm for MS-EVB simulations is described in greater detail in the Appendix. Simulations were performed using the DL_POLY molecular dynamics package (version 2.12) (Smith and Forester, 1996), which was modified to incorporate the MS-EVB2 model.

## RESULTS

### Equilibrium properties

First, the positions of the excess proton were explored with respect to the membrane surface. Due to the delocalized nature of the excess protonic charge, a suitable coordinate must be defined that describes the position of the "excess proton" at each step. The "center of excess charge" (CEC)

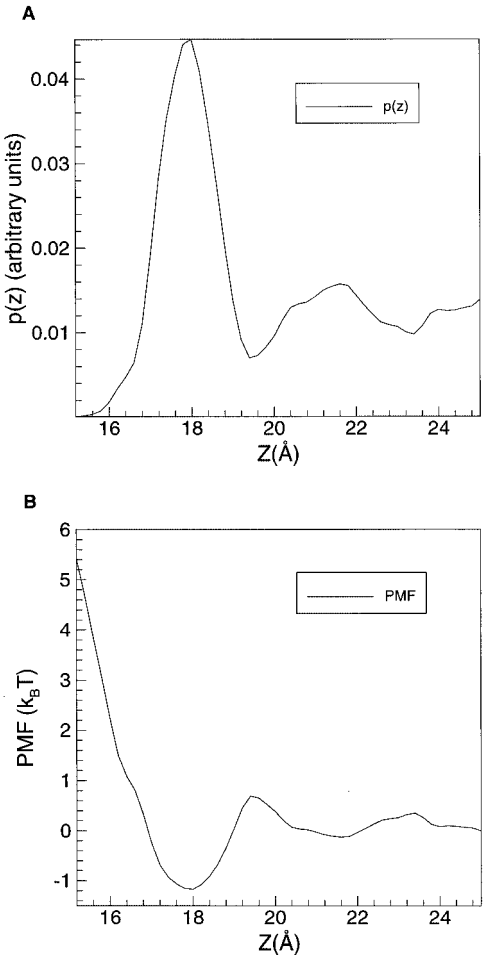


FIGURE 2 (*A*) The probability to find the center of excess charge of the proton at a given distance from the bilayer center (*top plot*); (*B*) PMF for the center of excess charge as a function of distance from the bilayer center (*solid line*). The middle of the membrane corresponds to $z = 0$. The barrier of 0.9 $k_BT$ in going from the solvent layer to the DMPC polar group region is seen in moving from $z \sim 22.0$ to 19.5 Å. The barrier in moving from the bilayer surface back to the solvent layer is seen as $z$ goes from $z \sim 18.0$ to 19.5 Å, having a value of 1.2 $k_BT$.

(Cuma et al., 2001) is one such coordinate, which is given by the vector:

$$R_{CEC}(t) = \sum_{i=1}^{N_{evb}} c_i^2 r_i(t), \quad (1)$$

in which $c_i$ is the component of the ground state eigenvector and $r_i(t)$ is the oxygen position vector of the hydronium in "$i$-th" MS-EVB state. The "pivot" oxygen $O^*$ is the oxygen atom from the hydronium state with the highest probability $c_i^2$.

The probability $p(z)$ to find the "excess proton" CEC at a particular distance ($z$) from the bilayer center is shown in Fig. 2 *A*, as a result of averaging over 2.0-ns MD runs. There is a distinct peak at approximately $z \sim 17.9$Å measured from the bilayer center, which is similar to the average

position of the phosphate groups (~17.1 ± 1.9 Å) (Smondyrev and Berkowitz, 1999a). This is likely due to the favorable interaction between the positively charged hydronium $H_3O^+$ and the negatively charged phosphate groups of DMPC. The hydronium density function decays rapidly towards the bilayer center and vanishes at approximately the same distance from the bilayer center as the DMPC carbonyl groups. The probability to find $H_3O^+$ in the solvent layer is almost uniform with a slightly higher tendency closer to the membrane surface.

One can also compute the potential of mean force (PMF) for the proton near the membrane surface using the following expression:

$$E_{\mathrm{PMF}}(z) = -k_{\mathrm{B}}T \ln p(z) + \mathrm{Const}, \qquad (2)$$

in which the integration constant Const is chosen so that the PMF is zero in the middle of the solvent layer (Fig. 2 *B*). As the proton approaches the DMPC polar group region in going from $z \sim 22.0$ to 19.5 Å the PMF increases by ~0.7 $k_{\mathrm{B}}T$.

Water molecules near the surface of the lipid bilayer have a highly ordered structure, which is due to both the electric field of the membrane (Essmann et al., 1995) and the presence of a hydrogen bonding network connecting the lipid's phosphate groups (Pasenkiewicz-Gierula et al., 1997). Thus some rearrangement of local hydrogen bonding network may be required as the proton diffuses towards the membrane surface. The energy barrier (Fig. 2 *B*) for the proton release from the bilayer surface back into the bulk solvent is ~1.2 $k_{\mathrm{B}}T$ in going from $z \sim 18.0$ to 19.5 Å. This higher barrier (compared with proton adsorption to membrane surface) may be due to the rearrangement of hydrogen bonds between hydronium and DMPC polar groups (see Discussion).

Simulations of DPPC bilayers in water have also shown that water molecules form a clathrate structure around choline moieties (Essmann et al., 1995). In Fig. 3 we show the pair distribution functions between oxygen atoms in the MS-EVB complex and the lipid atoms. It is evident that there is a strong affinity of hydronium towards phosphate groups. The first peak for the radial distribution function between phosphate and hydronium oxygens is located at ~3.9 Å for both the pivot water oxygen (*O**) and waters in the first solvation shell. This distance is similar to the one observed between phosphate and water P-OW, ~4.0 Å, in classical MD simulations (Smondyrev and Berkowitz, unpublished data). It should be noted that, as seen in Fig. 3, there is a higher probability to find the pivot hydronium oxygen close to phosphate compared with water oxygens in the first solvation shell.

The picture above is reversed for hydronium oxygens near the choline groups. The radial distribution functions shown in Fig. 3 for this case are almost structureless with a very diffuse first peak. There is a slightly higher probability

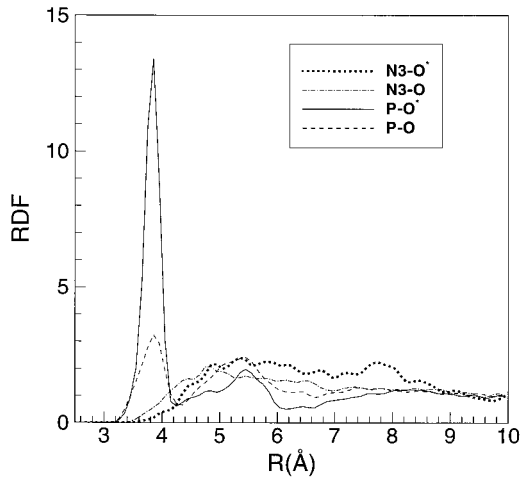


FIGURE 3 Pair distribution functions between the hydronium pivot oxygen *O** and lipid head group atoms: phosphorus (P) in phosphate group (*solid line*) and nitrogen (N3) in choline group (*dotted line*). Radial distribution functions between oxygens in the hydronium first solvation shell (O) and lipid headgroup atoms: P in phosphate group (*dashed line*) and N3 in choline group (*dash-dotted line*).

to find first solvation shell oxygens closer to a choline nitrogen compared with a pivot oxygen. This is in striking contrast with the results from classical simulations of PC bilayers in water (Essmann et al., 1995) where the well-defined clathrate structure was observed around choline groups with a well-defined first peak of the N-OW distribution at ~4.5 Å. The maximum of the radial distribution function between first solvation shell oxygens and choline nitrogen corresponds to ~4.8 Å.

As is evident from the radial distribution functions between the hydronium pivot oxygen and phosphate (Fig. 3), the pivot oxygen moves closer to negatively charged phosphate groups and forms a stable structure. The number of accessible EVB states is therefore reduced as the proton penetrates towards the bilayer center, reflecting a "stripping away" of the water solvation from the hydronium. Typical structures of hydronium in the membrane polar region are shown in Fig. 4 and exhibit two distinct motifs. First, an isolated hydronium forms one or two hydrogen bonds with lipid polar groups (phosphate and/or carbonyl groups). In this case the excess proton is more highly localized into a hydronium state with an amplitude of this state being $c_{\mathrm{o}}^2 \sim 0.8$ (Fig. 4 *A*). Second, two water molecules form hydrogen bonds with lipid polar group and share an excess proton, forming a Zundel cation (Fig. 4 *B*). Evidently, both structures are rather stable and prevent to some degree the release of an excess proton back into the bulk solvent.

## Proton diffusion

To characterize the diffusion of an excess proton, one can again consider the diffusion of the center of excess charge in

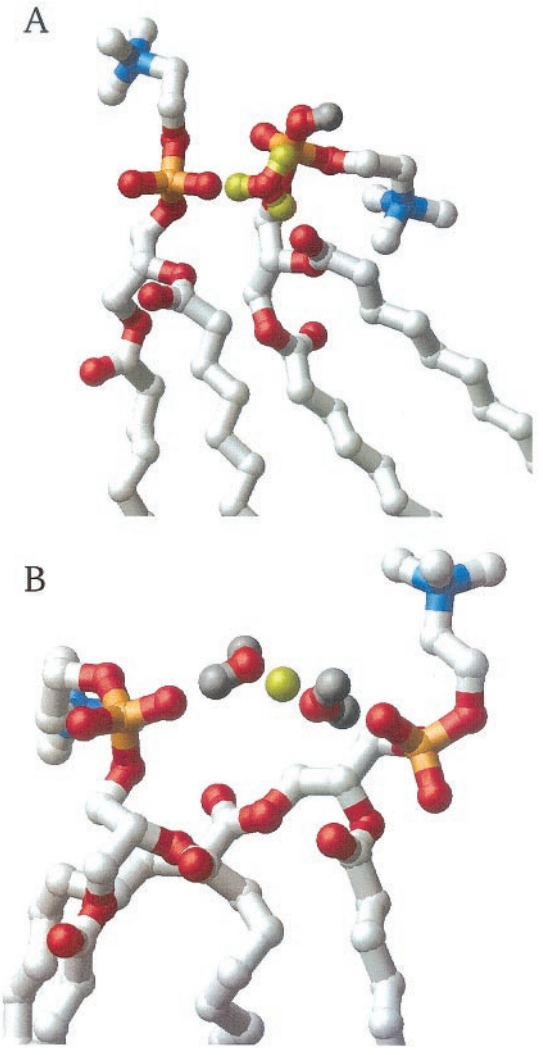


FIGURE 4 Snapshots of two representative configurations for the hydronium in the membrane polar region. (*A*) Hydronium molecule that forms two hydrogen bonds (one with the carbonyl group and another with the phosphate group) with two different lipids. The amplitude of this state is $c^2_{max} \sim 0.8$. (*B*) Zundel cation forming a bridge between phosphate groups of two adjacent lipid molecules. The excess proton is shared between two water molecules almost equally ($c^2_{max} \sim 0.5$).

Eq. 1. The diffusion constants were determined using the Einstein relation:

$$6Dt = |R_{CEC}(t) - R_{CEC}(0)|^2 \quad (3)$$

One can also calculate separate diffusion constants corresponding to motions along the membrane surface ($D_{lat}$) and along the bilayer normal ($D_n$). We can define three regions as a function of distance from the membrane surface. When the excess proton is far from the membrane surface ($z > 21$ Å) its mobility is similar to the one in bulk water ($3.5 \pm 1.2$) $\times 10^{-9}$ m$^2$/s (Cuma et al., 2001). The lateral and normal diffusion constants are ($3.4 \pm 0.1$) $\times 10^{-9}$ m$^2$/s and ($2.7 \pm 0.1$) $\times 10^{-9}$ m$^2$/s, correspondingly. We can see that

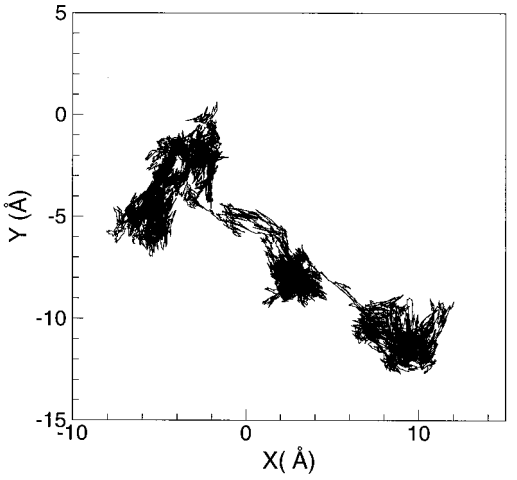


FIGURE 5 Representative trajectory of the center of excess charge diffusion along the surface of lipid membrane. For the duration of this simulation the excess proton did not become trapped in the polar group region nor did it diffuse entirely into the "bulk region" of the solvent layer. It can be seen that the excess proton diffuses rapidly between lipid molecules, whereas near the lipid headgroups it becomes more localized.

the diffusion along the bilayer normal is slightly inhibited compared with bulk water. As the proton penetrates into the membrane polar group region ($z < 19$ Å) it becomes more immobilized, as becomes evident from the diffusion constants: ($0.23 \pm 0.01$) $\times 10^{-9}$ m$^2$/s and ($0.14 \pm 0.01$) $\times 10^{-9}$ m$^2$/s for the lateral and normal constants, respectively. The third possibility arises as the proton diffuses close to the bilayer surface but does not become trapped in the polar group region of the membrane. A sample from a 160-ps trajectory is shown in Fig. 5. The excess proton diffuses rapidly between the adjacent lipids and becomes less mobile in their vicinity. As a result the lateral and normal diffusion constants have intermediate values compared to the two limiting regimes described above: ($1.9 \pm 0.1$) $\times 10^{-9}$ m$^2$/s and ($0.63 \pm 0.03$) $\times 10^{-9}$ m$^2$/s, respectively.

## MS-EVB amplitude analysis

The probability distribution of the largest EVB amplitude $c^2_{max}$ averaged over all trajectories for excess proton near the membrane surface is shown in Fig. 6. This distribution provides a convenient way to characterize the structure of solvated hydronium near the membrane surface. In bulk water, a value of $c^2_{max} \sim 0.7$ corresponds to an Eigen complex (Schmitt and Voth, 1999a,b). In the Zundel complex, two MS-EVB states share the excess proton almost equally, resulting in an amplitude $c^2_{max} \sim 0.5$. Clearly from Fig. 6, in the presence of a lipid bilayer the probability of Eigen cation formation decreases, whereas the probability of the Zundel complex increases. There is also a notable increase in the probabilities to find the complex with a larger amplitude $c^2_{max} > 0.7$, which indicates that the excess

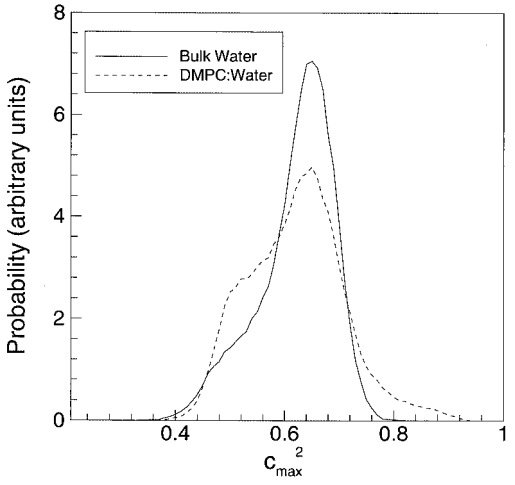


FIGURE 6 Probability distributions of the largest EVB amplitude $c^2_{max}$ for the excess proton in bulk water (*solid line*) and at the surface of the DMPC membrane (*dashed line*).

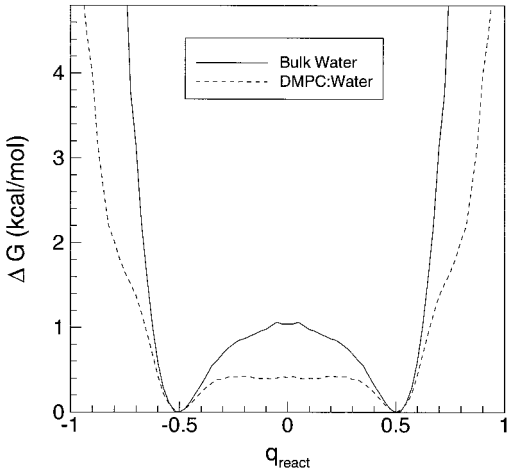


FIGURE 7 Free energy profiles as a function of reaction coordinate $q_{react}$ for the hydronium in water (*solid line*) and near the membrane surface (*dashed line*).

proton is more highly localized on a single hydronium state. Fig. 4 *B* shows one such complex, which has an amplitude $c^2_{max} \sim 0.8$. In this case, the hydronium forms two hydrogen bonds with lipid groups (one with carbonyl and another with phosphate groups of two adjacent lipid molecules) instead of water molecules. The typical number of MS-EVB states in such structures is 3 to 4, with one state having the dominant share of the total amplitude. It should be noted that the maximum amplitude probability distribution calculated using only trajectories where the hydronium is close to the middle of the solvent layer remains almost identical to the distributions obtained for bulk water (Schmitt and Voth, 1999a,b).

We can also consider the free energy profiles associated with a proton transfer "reaction coordinate" (Schmitt and Voth, 1999a), which can be conveniently defined as:

$$q_{react} = c_i^2 - c_j^2,$$

in which *i* and *j* are the indexes for the EVB states with two largest amplitudes. This coordinate is zero in case of Zundel cation and becomes $q_{react} \sim 0.5$ for the Eigen complex (in bulk water). Fig. 7 shows the free energy profile for the proton transfer near the membrane surface. The free energy for the formation of a Zundel complex becomes lower by ~0.6 (kcal/mol) compared with bulk water. A similar trend was also observed in simulations of water wires in a hydrophobic channel environment as the radius of the channel was decreased (Brewer et al., 2001). In the case of the excess proton at the membrane surface, the decrease in free energy may be due to the Zundel cation entering into the confined pockets at the membrane surface, as well as its interaction with the lipid's polar groups.

## CONCLUSIONS

In this paper results were presented from a molecular dynamics simulation of proton transport near the surface of a DMPC membrane. The proton hopping between water molecules was modeled using the MS-EVB2 potential energy surface. It was found that proton diffusion is significantly reduced as the proton penetrates into the polar region of the lipid membrane, which is also accompanied by significant changes in the structural properties of the hydronium-water complexes. The Zundel complex is seen to be more stabilized relative to the Eigen complex at the membrane surface compared with the bulk water case.

Two factors are likely to be responsible for the observed behavior of the excess proton. First, the proton moves into the confined pockets formed by the adjacent lipid molecules and along the rugged surface of the membrane. Thus, the Zundel complex stabilization may occur on the basis of geometric considerations. A similar mechanism was found in simulations of the excess proton in model channels with a variable radius (Brewer et al., 2001). Second, hydronium interacts with the polar headgroups of the lipid molecules and participates in the formation of "bridges" between adjacent lipid molecules, which in turn stabilizes such structures. It should be noted that stabilization of the Zundel complex is accompanied by a reduction in the total number of possible EVB states near the polar region of the lipid bilayer. It was found that the energy barrier for the proton transport from the membrane surface back into the bulk is ~1.2 $k_BT$, which is higher than the energy barrier for the proton adsorption to the membrane surface (~0.7 $k_BT$) (Fig. 2 *B*). Having moved away from the membrane surface, the proton diffusion constants within the solvent region are very similar to the ones observed in the bulk water.

More recently, Zahn and Brickmann performed a combined quantum-classical simulation of proton transport near a phospholipid bilayer composed of DLPE molecules (Zahn and Brickmann, 2001). The results of these simulations are in striking contrast with our findings. Zahn and Brickman reported an activation barrier of 20 kcal/mol for the proton adsorption into the membrane and a back diffusion activation barrier of 8 kcal/mol. Both of these values are an order of magnitude higher than the values reported in our work. It should be noted that the DLPE membrane differs in a number of ways from the DMPC membrane. First, the average area per DLPE molecule 46.8 $Å^2$ (Zahn and Brickmann, 2001) and 50 $Å^2$ (Damodaran and Merz, 1994) is smaller than the equilibrium area per DMPC molecule (60 $Å^2$ (Smondyrev and Berkowitz, 1999a)) (for a review of lipid bilayer structure, see Nagle and Tristram-Nagle, 2000). Thus, the average distances between adjacent lipid molecules is smaller in DLPE and can affect the headgroup conformations. One might expect that the lipid headgroups would be oriented more towards the solvent layer. A similar effect was observed in simulations of DPPC membranes in the liquid crystal and gel phase (Tu et al., 1996). As a result the water next to the membrane surface could be more polarized and this in turn could affect the activation barrier for the proton adsorption. Another possibility is that the observed behavior is due to the different and more approximate treatment of the proton transfer in the model of Zahn and Brickmann (2001) compared with the present work, as the excess charge in MS-EVB model is distributed over a larger number of water molecules due to the Grotthuss mechanism. It should also be noted that a number of real factors may have a profound effect on the hydronium interaction with biological membranes, such as membrane composition and the presence of various buffers in solution. In this context the observed differences for energy barriers in DLPE and DMPC membranes may require a detailed examination using a common modeling approach.

The diffusion constants obtained in this work are smaller than the values typically reported for experiments on various PC membranes ($\sim 9.0 \times 10^{-9}$ $m^2/s$) (Gutman et al., 1992). We also did not observe any enhancement in the diffusion rates for trajectories close to the membrane surface as has been suggested by some experimental measurements (Prats et al., 1985). Our results and the data of Zahn and Brickmann (2001) indicate that free energy profiles may be sensitive to the membrane composition. Our results do indicate, however, that hydronium has a higher affinity toward the DMPC membrane surface compared with bulk solvent. This result is consistent with experimental findings of an increased proton dwell time near the membrane surface (Nachliel and Gutman, 1996). It has also been suggested (Gutman et al., 1985; Junge and McLaughlin, 1987) that the presence of mobile buffers in the intermembrane solvent may have a significant effect on the proton diffusion. In the present work we did not introduce any mobile buffers into the solvent. The changes of proton mobility due to the membrane composition and the incorporation of various buffers into the solvent will be the topic of future research.

## APPENDIX

In this Appendix we will describe an efficient algorithm for the Ewald sum calculations for the MS-EVB model. It has been shown that certain artifacts can arise in simulations of bulk water due to the use of simple cutoff schemes in calculations of Coulombic energy (Hummer et al., 1997). These artifacts could be a serious issue in simulations using MS-EVB methodology, where the accurate calculation of EVB state energies is essential. The Ewald summation technique can resolve this problem. An essential feature of the MS-EVB model for proton transport in water is that it includes solvent-solute charge interactions in both the diagonal and off-diagonal elements of the EVB matrix. A straightforward application of the Ewald sum method would require $\sim 2 \times N$ Ewald calculations (where $N$ is the number of EVB states), which would be extremely computationally intensive especially in simulations of biological systems. The most expensive part of Ewald sum calculations is the $k$ space part of the Ewald sum, which is given by:

$$U_k = \frac{V}{2} \sum_{k \neq 0} \frac{4\pi}{k^2} |\rho(k)^2| \exp(-k^2/4\alpha), \tag{4}$$

in which we have defined $\rho(k)$ as:

$$\rho(k) = \frac{1}{V} \sum_{i=1}^{N_{atom}} q_i \exp(ikr_i), \tag{5}$$

and $q_i$ and $r_i$ are atomic charges and positions, respectively. The force contributions on atom "j" due to the $k$-space sum can be written as:

$$f_j = -\frac{1}{2V} \sum_{k \neq 0} \frac{4\pi}{k^2} \exp(-k^2/4\alpha) q_j (ik \exp(ikr_j)) \times \sum_{i=1}^{N_{atom}} q_i \exp(-ikr_i) \tag{6}$$

Here we propose the following computational scheme for the calculations of the $k$-space part in the Ewald sum: 1) First, we separate all atoms in the system into two sets: atoms that belong to EVB states at this timestep (set A) and the rest of the atoms in the system (set B). The main difference between the two sets is that the atomic charges in set B are constant, whereas the atomic charges in set A would be different for different EVB states. Now we can rewrite (Eq. 2) as:

$$\rho(k) = \rho^A(k) + \rho^B(k) = \frac{1}{V} \sum_{i=1}^{N_A} q_i \exp(ikr_i) + \frac{1}{V} \sum_{i=1}^{N_B} q_i \exp(ikr_i), \tag{7}$$

in which the first sum is taken over atoms in set A and the second for atoms in set B. We can note now that the sum over atoms in set B can be calculated only once, whereas the sum over atoms in set A should be calculated for each element of the EVB matrix. The energy contributions to the EVB matrix due to the $k$-space part of the Ewald sum can be calculated separately from forces and used to calculate the components of the ground state eigenvector $c_i^0$. This would be used later to perform efficient calculations of force contributions due to the $k$-space term in the Ewald sum.

2) We can use a similar strategy in calculations of forces, namely separate the last sum in Eq. 6 into two contributions: sum over atoms in sets A and B. Thus, the force on atom "j" can be written as:

$$f_j = -\frac{1}{2V}\sum_{k\neq 0}\frac{4\pi}{k^2}\exp(-k^2/4\alpha)\times q_j(ik\exp(ikr_j))\times(\rho^A(-k)+\rho^B(-k)) \quad (8)$$

Now we can calculate force contributions in several steps. First, if atom "j" belong to set B the term involving $q_j(ik\exp(ikr_j))\times\rho^B(-k)$ would depend only on charges in set B and thus would be the same for all EVB matrix elements. It can be calculated only once per MD step. The other term is proportional to $q_j(ik\exp(ikr_j))\times\rho^A(-k)$ and should be, in principal, calculated for each element of the EVB matrix. However we can use the fact that this term is linear with respect to charges on atoms in set A. According to the Hellmann-Feynman theorem the final force can be written as:

$$F_i = \sum_{m,n} c_m^0 c_n^0 f_i^{mn}, \quad (9)$$

in which $f_i^{mn}$ is the force on atom *i* due to the potential of the (*m*, *n*) matrix element in the EVB matrix. Now we can introduce an effective EVB charge on atom *i* as:

$$q_i' = \sum_{m,n} c_m^0 c_n^0 q_i^{mn}, \quad (10)$$

in which $q_i^{mn}$ is the charge on atom *i*, corresponding to matrix element (*m*, *n*) in the EVB matrix. The effective EVB charges $q_i'$ can be then used to calculate the $\rho^A(-k)$ term and thus perform only one Ewald sum calculation to obtain contributions to forces. The second possibility is when atom "j" belongs to set A. The term in Eq. 8, which is proportional to $q_j(ik\exp(ikr_j))\times\rho^A(-k)$ has to be calculated for each element of the EVB matrix. However, in a typical biological simulation the total number of atoms in the system is several thousand atoms, whereas the maximum number of atoms in the EVB complex is typically ~20 to 40. Thus, the calculation of this term would represent only a small fraction of the Ewald sum calculation. The last term, which is proportional to $q_j(ik\exp(ikr_j))\times\rho^B(-k)$, also has to be calculated for each element of the EVB matrix, but the term $\rho^B(-k)$ is the same for all EVB matrix elements, and its calculation is not computationally intensive. Again, an "effective EVB charge" $q_j'$ can be used in place of $q_j$ resulting in a single Ewald calculation.

To summarize the algorithm outlined above, we separate the calculation of the *k*-space part in the Ewald sum into several steps. First, we separate all atoms in the system into two sets: EVB complex atoms and the rest of the atoms. Second, we calculate only energy contributions to the EVB Hamiltonian matrix and calculate the ground state eigenvector. Part of the forces due to the *k*-space sum is also calculated for each EVB matrix element. We can now define the effective charges on atoms belonging to set A according to Eq. 10 and use them to calculate the remaining contribution to forces by performing only a single Ewald calculation. Our benchmark results for a system consisting of ~7000 atoms indicate that the main contribution due to the incorporation of EVB comes from the one additional calculation of the *k*-space part of the Ewald sum. Computational efforts required to calculate energy contributions to the EVB matrix are almost negligible. This presents an opportunity to perform simulations using Ewald summation with the MS-EVB model, which takes into account a larger number of EVB states or contains several protons.

This work was supported by the grant from the National Institutes of Health (GM-53148). Computational support from the Pittsburgh Supercomputing Center, The National Center for Supercomputing Applications, and The Utah Center for High Performance Computing is gratefully acknowledged. We thank Martin Cuma, Udo Schmitt, and Tyler Day for helpful discussions.

## REFERENCES

Agmon, N. 1995. The Grotthuss mechanism. *Chem. Phys. Lett.* 244: 456–462.

Brandsburg-Zabary, S., O. Fried, Y. Marantz, E. Nachliel, and M. Gutman. 2000. Biophysical aspects of intra-protein proton transfer. *Biochim. Biophys. Acta.* 1458:120–134.

Brewer, M. L., U. W. Schmitt, and G. A. Voth. 2001. The formation and dynamics of proton wires in channel environments. *Biophys. J.* 80: 1691–1702.

Car, R., and M. Parrinello. 1985. Unified approach for molecular dynamics and density-functional theory. *Phys. Rev. Lett.* 55:2471–2474.

Cuma, M., U. W. Schmitt, and G. A. Voth. 2001. A multi-state empirical valence bond model for weak acid dissociation in aqueous solution. *J. Phys. Chem. A.* 105:2814–2823.

Damodaran, K. V., and K. M. Merz. 1994. A comparison of DMPC- and DLPE-based lipid bilayers. *Biophys. J.* 66:1076–1087.

Dang, L. X., and B. M. Pettitt. 1987. Simple intermolecular model potentials for water. *J. Phys. Chem.* 91:3349.

Deamer, D. W. 1996. Water chains in lipid bilayers. *Biophys. J.* 71:543.

Dubos, R. J., and R. D. Hotchkiss. 1941. The production of bactericidal substances by aerobic sporulating bacilli. *J. Exp. Med.* 73:629–640.

Essmann, U., L. Perera, and M. L. Berkowitz. 1995. The origin of the hydration interaction of lipid bilayers from MD simulation of dipalmitoylphosphatidylcholine membranes in gel and liquid crystalline phases. *Langmuir.* 11:4519–4531.

Futai, M., T. Noumi, and M. Maeda. 1989. ATP synthase ($H^+$-ATPase) results of combined biochemical and molecular biological approaches. *Annu. Rev. Biochem.* 58:111–136.

Gutman, M., E. Nachliel, and E. Gershon. 1985. Effect of buffer on kinetics of proton equilibration with a protonable group. *Biochemistry.* 24:2937–2941.

Gutman, M., E. Nachliel, and S. Kiryati. 1992. Dynamic studies of proton diffusion in mesoscopic heterogeneous matrix: II The interbilayer space between phospholipid membranes. *Biophys. J.* 63:281–290.

Heberle, J. 2000. Proton transfer reactions across bacteriorhodopsin and along the membrane. *Biochim. Biophys. Acta.* 1458:135–147.

Heberle, J., and N. A. Dencher. 1992. Surface-bound optical probes monitor proton translocation and surface potential changes during the bacteriorhodopsin photocycle. *Proc. Natl. Acad. Sci. U.S.A.* 89:5996–6000.

Heberle, J., J. Riesle, G. Thiedemann, D. Oesterhelt, and N. A. Dencher. 1994. Proton migration along the membrane surface and retarded surface to bulk transfer. *Nature.* 370:379–382.

Hoover, W. G. 1985. Canonical dynamics: equilibrium phase-space distributions. *Phys. Rev. A.* 31:1695–1697.

Hummer, G., L. R. Pratt, A. E. Garcia, B. J. Berne, and S. W. Rick. 1997. Electrostatic potentials and free energies of solvation for polar and charged molecules. *J. Phys. Chem.* 101:3017–3020.

Junge, W., and S. McLaughlin. 1987. The role of fixed and mobile buffers in the kinetics of proton movement. *Biochim. Biophys. Acta.* 890:1–5.

Lill, M. A., and V. Helms. 2001. Molecular dynamics simulation of proton transport with quantum mechanically derived proton hopping rates (Q-HOP MD). *J. Chem. Phys.* 115:7993–8005.

Lobaugh, J., and G. A. Voth. 1996. The quantum dynamics of an excess proton in water. *J. Chem. Phys.* 104:2056–2069.

Malmstrom, B. G. 1989. The mechanism of proton translocation in respiration and photosynthesis. *FEBS Lett.* 250:9–21.

Marrink, S. J., F. Jahnig, and H. J. C. Berendsen. 1996. Proton transport across transient single-file water pores in a lipid membrane studied by molecular dynamics simulations. *Biophys. J.* 71:632–647.

Marx, D., M. E. Tuckerman, J. Hutter, and M. Parrinello. 1999. The nature of the hydrated proton in water. *Nature.* 397:601–604.

Mathies, R. A., S. W. Lin, J. B. Ames, and W. T. Pollard. 1991. From femtoseconds to biology: mechanism of bacteriorhodopsin's light-driven proton pump. *Annu. Rev. Biophys. Biophys. Chem.* 20:491–518.

Nachliel, E., and M. Gutman. 1996. Quantitative evaluation of the dynamics of proton transfer from photoactivated bacteriorhodopsin to the bulk. *FEBS Lett.* 393:221–225.

Nagle, J. F., and R. A. Dilley. 1986. Models of localized energy coupling. *J. Bioenerg. Biomembr.* 18:55–64.

Nagle, J. F., and S. Tristram-Nagle. 1983. Hydrogen bonded chain mechanisms for proton conduction and proton pumping. *J. Membr. Biol.* 74:1–14.

Nagle, J. F., and S. Tristram-Nagle. 2000. Structure of lipid bilayers. *Biochim. Biophys. Acta.* 1469:159–195.

Nagle, J. F., and M. C. Weiner. 1988. Structure of fully hydrated bilayer dispersions. *Biochim. Biophys. Acta.* 942:1–10.

Pasenkiewicz-Gierula, M., Y. Takaoka, H. Miyagawa, K. Kitamura, and A. Kusumi. 1997. Hydrogen bonding of water to phosphatidylcholine in the membrane as studied by a molecular dynamics simulation: location, geometry, and lipid-lipid bridging via hydrogen-bonded water. *J. Phys. Chem.* 101:3677–3691.

Prats, M., J. F. Tocanne, and J. Teissie. 1985. Lateral proton conduction at lipid/water interface: its modulation by physical parameters, experimental and mathematical approaches. *Eur. J. Biochem.* 149:663–668.

Ryckaert, W. E., G. Ciccotti, and H. J. C. Berendsen. 1977. Numerical integration of the cartesian equations of motion of a system with constraints: molecular dynamics of *n*-alkanes. *J. Comput. Phys.* 23: 327–341.

Scherrer, P., U. Alexiev, T. Marti, H. Gobind Khorana, and M. P. Heyn. 1994. Covalently bound pH-indicator dyes at selected extracellular of cytoplasmic sites in bacteriorhodopsin: I. Proton migration along the surface of bacteriorhodopsin micelles and its delayed transfer from surface to bulk. *Biochemistry.* 33:13684–13692.

Schmitt, U. W., and G. A. Voth. 1998. Multistate empirical valence bond model for proton transport in water. *J. Phys. Chem. B.* 102:5547.

Schmitt, U. W., and G. A. Voth. 1999a. The computer simulation of proton transportin water. *J. Chem. Phys.* 111:9361.

Schmitt, U. W., and G. A. Voth. 1999b. Quantum properties of the excess proton in liquid water. *Isr. J. Chem.* 39:483.

Schumaker, M. F., R. Pomes, and B. Roux. 2000. A combined molecular dynamics and diffusion model of single proton conduction through gramicidin. *Biophys. J.* 79:2840–2857.

Schumaker, M. F., R. Pomes, and B. Roux. 2001. Framework model for single proton conduction through gramicidin. *Biophys. J.* 80:12–30.

Smith, W., and T. R. Forester. 1996. DL_POLY is a package of molecular simulation routines written by W. Smith and T. R. Forester. Copyright The Council for the Central Laboratory of the Research Councils, Daresbury Laboratory at Daresbury, Nr. Warrington.

Smondyrev, A. M., and M. L. Berkowitz. 1999a. Molecular dynamics simulation of fluorination effects on a phospholipid bilayer. *J. Chem. Phys.* 111:9864–9870.

Smondyrev, A. M., and M. L. Berkowitz. 1999b. United atom force field for phospholipid membranes: constant pressure molecular dynamics simulation of DPPC/water system. *J. Comp. Chem.* 20:531–545.

Sugrue, R. J., and A. J. Hay. 1991. Structural characteristics of the M2 protein of influenza A viruses: evidence that it forms tetrameric channel. *Virology.* 180:617–624.

Tu, K., D. J. Tobias, and M. L. Klein. 1996. Molecular dynamics investigation of the structure of a fully hydrated gel-phase dipalmitoylphosphatidylcholine bilayer. *Biophys. J.* 70:595.

Vuilleumier, R., and D. Borgis. 1997. Molecular dynamics of an excess proton in water using a non-additive valence bond force field. *J. Mol. Struct.* 436:555.

Vuilleumier, R., and D. Borgis. 1998a. An extended valence bond model for describing proton transfer in $H^+(H_2O)_n$ clusters and liquid water. *Chem. Phys. Lett.* 284:71.

Vuilleumier, R., and D. Borgis. 1998b. Quantum dynamics of an excess proton in water using an extended empirical valence-bond Hamiltonian. *J. Phys. Chem.* 102:4261–4264.

Vuilleumier, R., and D. Borgis. 1999. Transport and spectroscopy of the hydrated proton: a molecular dynamics study. *J. Chem. Phys.* 111: 4251–4266.

Walbran, S., and A. A. Kornyshev. 2001. Proton transport in polarizable water. *J. Chem. Phys.* 114:10039–10048.

Zahn, D., and J. Brickmann. 2001. Quantum-classical simulation of proton transport via a phospholipid bilayer. *Phys. Chem. Chem. Phys.* 3:848–852.